




BRIEF COMMUNICATION

# Mouse Model of Heart Failure With Preserved Ejection Fraction Driven by Hyperlipidemia and Enhanced Cardiac Low-Density Lipoprotein Receptor Expression

Monique Williams, MD; Jose Manuel Condor Capcha, PhD; Camila Iansen Irion, PhD; Grace Seo, MS; Guerline Lambert, BS; Ali Kamiar , PharmD; Keyvan Yousefi, PharmD, PhD; Rosemeire Kanashiro-Takeuchi, PhD, DVM; Lauro Takeuchi, DDS; Ali G. Saad, MD; Armando Mendez, PhD; Keith A. Webster, PhD; Jeffrey J. Goldberger , MD; Joshua M. Hare, MD; Lina A. Shehadeh , PhD

**BACKGROUND:** The pathways of diastolic dysfunction and heart failure with preserved ejection fraction driven by lipotoxicity with metabolic syndrome are incompletely understood. Thus, there is an urgent need for animal models that accurately mimic the metabolic and cardiovascular phenotypes of this phenogroup for mechanistic studies.

**METHODS AND RESULTS:** Hyperlipidemia was induced in WT-129 mice by 4 weeks of biweekly poloxamer-407 intraperitoneal injections with or without a single intravenous injection of adeno-associatedvirus 9–cardiac troponin T–low-density lipoprotein receptor (n=31), or single intravenous injection with adeno-associatedvirus 9–cardiac troponin T–low-density lipoprotein receptor alone (n=10). Treatment groups were compared with untreated or placebo controls (n=37). Echocardiography, blood pressure, whole-body plethysmography, ECG telemetry, activity wheel monitoring, and biochemical and histological changes were assessed at 4 to 8 weeks. At 4 weeks, double treatment conferred diastolic dysfunction, preserved ejection fraction, and increased left ventricular wall thickness. Blood pressure and whole-body plethysmography results were normal, but respiration decreased at 8 weeks ( $P<0.01$ ). ECG and activity wheel monitoring, respectively, indicated heart block and decreased exercise activity ( $P<0.001$ ). Double treatment promoted elevated myocardial lipids including total cholesterol, fibrosis, increased wet/dry lung ( $P<0.001$ ) and heart weight/body weight ( $P<0.05$ ). Xanthelasma, ascites, and cardiac ischemia were evident in double and single (p407) groups. Sudden death occurred between 6 and 12 weeks in double and single (p407) treatment groups.

**CONCLUSIONS:** We present a novel model of heart failure with preserved ejection fraction driven by dyslipidemia where mice acquire diastolic dysfunction, arrhythmia, cardiac hypertrophy, fibrosis, pulmonary congestion, exercise intolerance, and preserved ejection fraction in the absence of obesity, hypertension, kidney disease, or diabetes. The model can be applied to dissect pathways of metabolic syndrome that drive diastolic dysfunction in this lipotoxicity-mediated heart failure with preserved ejection fraction phenogroup mimic.

**Key Words:** heart failure ■ hyperlipidemias ■ mice ■ stroke volume

**W**ith a high and increasing incidence and few effective treatment options, heart failure with preserved ejection fraction (HFpEF) has been designated the greatest unmet medical need in cardiovascular disease.<sup>1</sup> HFpEF accounts for  $\geq 50\%$  of HF

diagnoses worldwide, and its complex cause reflects a multisystem as opposed to monolithic disease.<sup>1</sup> Animal models, which are required to dissect the underlying pathophysiology and identify therapeutic targets for HFpEF, must be similarly multifactorial and reflect

Correspondence to: Lina Shehadeh, PhD, Biomedical Research Building Rm 824, The University of Miami, Miller School of Medicine, 1501 NW 10th Ave, Miami, FL 33136. Email: [lshehadeh@med.miami.edu](mailto:lshehadeh@med.miami.edu)

For Sources of Funding and Disclosures, see page 5.

© 2022 The Authors. Published on behalf of the American Heart Association, Inc., by Wiley. This is an open access article under the terms of the [Creative Commons Attribution-NonCommercial](#) License, which permits use, distribution and reproduction in any medium, provided the original work is properly cited and is not used for commercial purposes.

JAHA is available at: [www.ahajournals.org/journal/jaha](http://www.ahajournals.org/journal/jaha)

individual human classes of the disease. Tied with hypertension as the third most important independent risk factor after age and sex, obesity-driven HFpEF represents a distinct pathophysiological phenotype wherein direct cardiac lipotoxicity may confer cardiac dysfunction.<sup>2</sup> The precise mechanisms involved in diastolic dysfunction driven by excess accumulation of myocardial lipids are unclear and animal models are few.<sup>3</sup> Lipoprotein lipase (LPL) is decreased (Figure 1A) and low-density lipoprotein receptor (LDLR) increased in patients with HFpEF.<sup>4,5</sup> Here we describe a novel, reproducible mouse model of rapid-onset HFpEF wherein hyperlipidemia conferred by pharmacologic inhibition of LPL by poloxamer-407 (P407), a selective LPL inhibitor, and cardiac-specific overexpression of the LDLR drive a full spectrum of classic symptoms that are independent of hypertension, diabetes, or kidney disease.

## METHODS

The data that support the findings of this study are available from the corresponding author upon reasonable request. All procedures involving animals were approved by the Institutional Animal Care and Use Committee at the University of Miami, conforming to National Institutes of Health guidelines (IACUC protocol 20–118). Wild type (WT) mice on 129/J background were subjected to biweekly intraperitoneal injections of poloxamer-407 with or without a single intravenous injection of  $1 \times 10^{12}$  VGS adeno-associatedvirus 9–cardiac troponin T-LDLR to direct human LDLR overexpression selectively to the heart. Controls received single, placebo, or no treatment. At 4 weeks and 8 weeks post-treatment, echocardiography, whole body plethysmography, tail-cuff blood pressure recording,

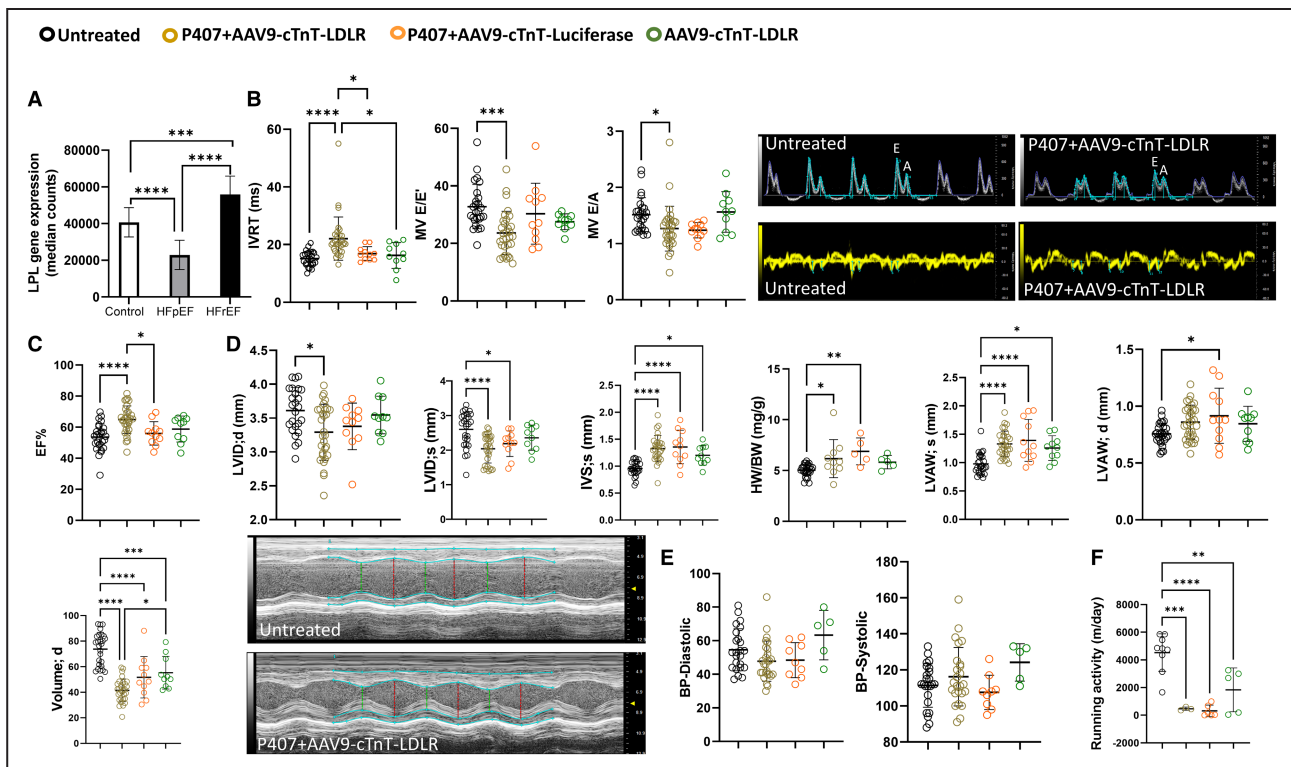


**Figure 1.** Heart failure with preserved ejection fraction features with normal blood pressure were shown by the double treatment mice.

**A**, Representative graph comparing lipoprotein lipase (LPL) gene expression in endomyocardial biopsies obtained from healthy human controls ( $n=24$ ), patients with heart failure with preserved ejection fraction (HFpEF,  $n=41$ ), and heart failure with reduced ejection fraction (HFrEF,  $n=30$ ) shows decreased LPL in patients with HFpEF (RNA sequencing data from Hahn et al).<sup>4</sup> **B**, Representative echocardiography images showing diastolic dysfunction predominantly in the double-treatment group ( $n=31$ ) as evidenced by prolonged isovolumic relaxation time (IVRT), decreased MV E/A and MV E/E' compared with untreated ( $n=26$ ), 407+Adeno-associatedvirus9–cardiac troponin T–Luciferase (AAV9-cTnT-Luciferase,  $n=11$ ) and Adeno-associatedvirus9–cardiac troponin T–LDL receptor (AAV9-cTnT-LDLR,  $n=10$ ) groups. **C**, Echocardiography revealed preserved ejection fraction (EF%) in all treatment groups. **D**, Representative graphs showing features of left ventricular hypertrophy; increased left ventricular anterior wall thickness (LVAW), heart weight/body weight (HW/BW), and decreased left ventricular internal diameter (LVID) and volume. IVS indicates interventricular septum. **E**, Representative graphs reveal normal diastolic and systolic blood pressures (BP) in each group. **F**, Representative graphs showing daily running activity decreased in all groups; the poloxamer-407+AAV9-cTnT-Luciferase ( $n=6$ ) group showed the lowest activity ( $P<0.0001$ ) followed by the double-treatment ( $n=3$ ;  $P<0.001$ ) and AAV9-cTnT-LDLR ( $n=5$ ;  $P<0.01$ ). For all analyses (except total cholesterol and triglyceride analyses comparing 2 groups by  $t$  test), 2-way ANOVA with Tukey–Kramer post hoc correction was used. In all figure panels, means $\pm$ SD was used. \* $P<0.05$ ; \*\* $P<0.01$ ; \*\*\* $P<0.001$ ; and \*\*\*\* $P<0.0001$ .

voluntary wheel exercise, ECG telemetry, and histology were performed. Cardiac morphology and function was assessed using the Vevo2100 imaging system (Visual Sonics, Toronto, ON, Canada) with a MS400 linear array transducer (as in our previous work<sup>6</sup>). Blood pressure was recorded using a noninvasive tail-cuff method (BP-2000 Series II, Visitech Systems, Apex, NC). Mice were trained for 4 consecutive days and data were collected on day 5 (as in our previous work<sup>6</sup>). Respiratory function was assessed using a Buxco small animal whole body plethysmography system and FinePoint software (Data Science International, New Brighton, MN). Mice were acclimatized for 3 consecutive days and data were collected on day 4 (as in our previous work<sup>6</sup>). Activity wheel monitoring was assessed using Lafayette Instrument Activity Wheel Monitor Model 86056 (Lafayette Instrument, Lafayette, IN) (as in our previous work<sup>7</sup>). Mice were acclimatized for 2 days and data were collected over 5 days. Electrocardiogram data were obtained from radiotelemetry HD-X11 ECG devices (Data Science International, St. Paul, MN).

### Statistical Analysis

Two-way ANOVA with Tukey–Kramer post hoc correction was used for all 4-group experiments. Student *t* test was used to analyze results from 2-group experiments. For survival curve analysis, the Log-rank test was used. A significance level of  $P < 0.05$  was used and all tests are 2-sided. All data are presented as means  $\pm$  SD. GraphPad Prism 9 software was used for all the analyses and graph generations.

## RESULTS

Elevated myocardial lipids is a prominent feature of patients with HFpEF<sup>3</sup> and the gene for LPL in cardiac biopsies is decreased compared with HFrEF or healthy controls.<sup>4</sup> Poloxamer-407 induces hyperlipidemia by blocking LPL and increasing plasma triglycerides and LDL cholesterol.<sup>8</sup> Our group recently reported that LDLR levels are increased in autopsy specimens of hearts from sudden cardiac death victims with HFpEF and diabetes.<sup>5</sup> We hypothesized that hyperlipidemia driven by poloxamer-407 and overexpression of cardiac LDLR in mice mimics the subset of human HFpEF, where metabolic syndrome and diastolic dysfunction are driven primarily by lipotoxicity.<sup>3</sup> Quantitative polymerase chain reaction, Western blot, and immunostaining confirmed >3-fold overexpression of LDLR in hearts 4 weeks after injection of adeno-associated virus9–cardiac troponin T–LDLR (data not shown). Echocardiography of double-treatment mice at 4 weeks revealed diastolic dysfunction as evidenced by prolonged isovolumic relaxation time, decreased MV E/A and MV E/E' (Figure 1B) and preserved EF (Figure 1C). Echocardiography also

confirmed decreased left ventricular internal diameter (LVID;d and LVID;s), and increased interventricular septum and left ventricular anterior wall (LVAW) thickness (Figure 1D); the latter parameters were also increased in single-treatment groups. Blood pressure remained unchanged by treatments (Figure 1E), exercise intolerance was confirmed by decreased daily running distance in all groups (Figure 1F), and all mice remained nonobese. Telemetry/ECG revealed paroxysmal heart block coincident with lipid accumulation in the atrioventricular junction (Figure 2A), also a feature of human HFpEF.<sup>9</sup> Picrosirius Red staining confirmed the presence of fibrosis (Figure 2B). Galectin-3 is an early indicator of cardiac fibrosis and ventricular remodeling in patients with HF.<sup>10</sup> Galectin-3 was significantly elevated in the hearts of double-treatment mice compared with single-treatment or control groups (Figure 2B). Wheat germ agglutinin staining revealed significantly increased cell size in both double- and single-treatment groups, confirming cardiac hypertrophy (Figure 2C), and pulmonary congestion, a key manifestation of the clinical syndrome of HF, was indicated by increased lung wet/dry ratio (Figure 2D). Myocardial tissue from double-treatment mice contained increased cholesterol and decreased triglycerides, consistent with increased LDL-cholesterol uptake (Figure 2E). Total cholesterol was elevated in skeletal muscle and liver; triglycerides were reduced in liver while plasma glucose, blood urea nitrogen, and creatinine remained unchanged (data not shown). Hyperlipidemic mice succumbed to sudden death between 6 and 12 weeks of age (Figure 3A) irrespective of sex, and mice that survived 8 weeks developed more prominent phenotypes while preserving EF (data not shown). With an incidence of  $\approx 35\%$ , sudden death is a leading cause of HFpEF death.<sup>1</sup> At 8 weeks, decreased respiration rate was observed in the double-treatment group only (Figure 3B). Necropsy of double-treatment mice revealed pulmonary congestion and ascites, and cardiac ischemia (Figure 3C). Pulmonary hypertension and right ventricular dysfunction are often associated with HFpEF accompanied by hepatic venous congestion and hypoxemia.<sup>11</sup> The observed ascites is most likely a consequence of worsening HF and hepatic venous congestion. Unilateral and bilateral skin discoloration and deposits surrounding the eyelids suggest xanthelasmas, a consequence of hyperlipidemia.<sup>12</sup> In addition, at 8 weeks, free myocardial cholesterol was significantly increased in this group (Figure 3D).

## DISCUSSION

Together, the results provide a unique model of early-onset, rapidly progressing, hyperlipidemia-driven HFpEF where treated mice display diastolic dysfunction, arrhythmia, cardiac hypertrophy and fibrosis, pulmonary congestion and exercise intolerance, with

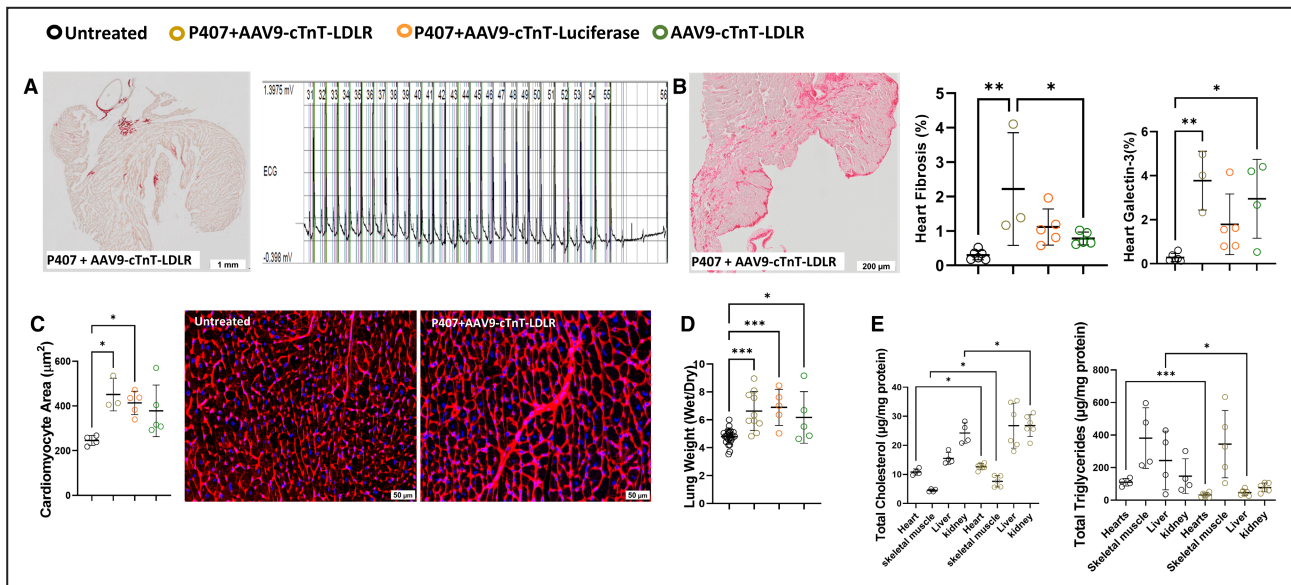


**Figure 2. Paroxysmal heart block coincident with cardiac lipid accumulation and fibrosis was evident in the double treatment mice.**

**A**, Representative images showing lipid accumulation at the atrioventricular junction in Oil Red O staining in the double-treatment group. Telemetry ECG tracing shows paroxysmal heart block in the double-treatment group. **B**, Representative Picrosirius Red staining image and quantitative graphs showing increased cardiac fibrosis and galectin in the double-treatment group ( $n=3$ ;  $P<0.01$ ) compared with the untreated ( $n=6$ ), poloxamer 407+Adeno-associatedvirus9-cardiac troponinT-Luciferase (AAV9-cTnT-Luciferase,  $n=5$ ) and Adeno-associatedvirus9-cardiac troponinT-low-density lipoprotein receptor (AAV9-cTnT-LDLR,  $n=5$ ) groups. **C**, Representative wheat germ agglutinin staining images and quantitative graph showing increased cardiomyocyte area in the double-treatment group ( $n=3$ ) compared with the untreated ( $n=6$ ;  $P=0.0178$ ), poloxamer-407+AAV9-cTnT-Luciferase ( $n=5$ ) and AAV9-cTnT-LDLR ( $n=5$ ) groups. **D**, Representative graph showing increased lung weight (wet/dry) in all groups but most significantly in the double-treatment ( $n=10$ ) and p407+AAV9-cTnT-Luciferase group ( $n=5$ ;  $P<0.001$ ) compared with the AAV9-cTnT-LDLR group ( $n=5$ ;  $P=0.0455$ ) and untreated group ( $n=25$ ), indicating pulmonary hypertension. **E**, Representative graphs showing biochemical results; the total cholesterol was increased in the hearts, skeletal muscles, and liver of the mice in the double-treatment group ( $n=6$ ) compared with untreated mice ( $n=4$ ); the total triglycerides were decreased in only the hearts and liver of these mice. The  $t$  test was used to analyze data. For all analyses, 2-way ANOVA with Tukey-Kramer post hoc correction was used. In all figure panels, means $\pm$ SD was used. \* $P<0.05$ ; \*\* $P<0.01$ ; and \*\*\* $P<0.001$ .

preserved EF, absence of hypertension and high incidence of sudden death, independent of kidney disease or diabetes. The model provides an opportunity to dissect the roles of hyperlipidemia driven by suppressed LPL and increased LDLR, both features of human HFpEF in the absence of hypertension or obesity and comorbidities related to diabetes and/or chronic kidney disease. The dramatic response of mice to the double-treatment regimen suggests that LDLR overexpression may exert pathophysiological effects beyond those restricted to LDL/cholesterol transport. In terms of phenotypes, our model bears similarity to a recently presented model of mice exposed simultaneously to high-fat diet and  $N^{\omega}$ -nitro- $L$ -arginine methyl ester to simulate metabolic stress and hypertension wherein the mice develop HFpEF over a period of 5 to 15 weeks.<sup>13</sup> Importantly, this work identified a defective unfolded protein response driven by inducible nitric oxide synthase as central to the HFpEF phenotype in treated mice. Pharmacological or genetic suppression of inducible nitric oxide synthase ameliorated

the phenotype. Key differences between our model and the  $N^{\omega}$ -nitro- $L$ -arginine methyl ester model include more rapid onset, absence of hypertension, presence of arrhythmias, higher and earlier incidence of sudden death, and absence of the potentially confounding effects of  $N^{\omega}$ -nitro- $L$ -arginine methyl ester that do not mimic the pathophysiology of hypertension in human HFpEF (reviewed in<sup>1</sup>). Also we observed no significant differences between sexes in treated mice, consistent with the possibility that sex-related differences in adipose deposition contribute to HFpEF in obese humans. We do not expect significant coronary artery disease as a factor in sudden death in this model because aortic atherosclerotic lesions in P-407-treated mice require >4 months to mature to mimic human-like pathological features.<sup>2</sup> Our model represents a unique subtype of HFpEF and presents an opportunity to dissect the pathways of hyperlipidemia and associated lipotoxicity in disease progression in the absence of hypertension, chronic kidney disease, diabetes, or obesity. Both models provide opportunities to further

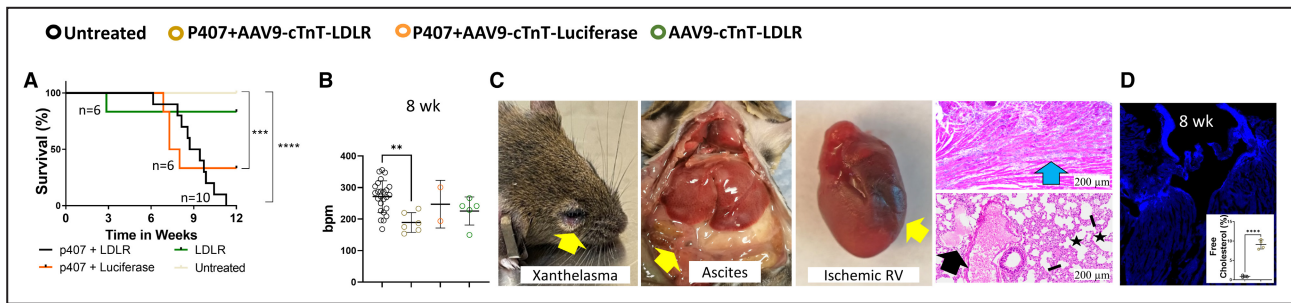


**Figure 3. Sudden death was predominant in the double treatment mice.**

**A**, Survival curve shows sudden deaths predominantly in both the poloxamer-407 (p407)+Adeno-associatedvirus9–cardiac troponin T–low-density lipoprotein receptor (AAV9–cTnT–LDLR) and p407+Adeno-associatedvirus9–Luciferase groups before 12 weeks. Log-rank test was used. **B**, Whole-body plethysmography revealed significantly decreased respiration rate (breaths per minute [bpm]) at 8 weeks in the p407+LDLR group (n=6) only compared with untreated (n=25), poloxamer 407+AAV9–cTnT–Luciferase (n=2) and AAV9–cTnT–LDLR (n=5) groups. Two-way ANOVA with Tukey–Kramer post hoc correction was used. **C**, Representative images showing xanthelasma, ascites, and ischemic right ventricle (RV) in mice from the double-treatment group that died suddenly; hematoxylin and eosin staining revealed myocardial infarction (blue arrow), pulmonary edema (black arrow); thick interalveolar septae (black lines), and emphysematous change (black stars). **D**, Representative image of Filipin staining and graph showing significantly increased free myocardial cholesterol at 8 weeks in the p407+LDLR group only. *T* test was used. In all figure panels, means±SD was used. \*\**P*<0.01; \*\*\**P*<0.001; and \*\*\*\**P*<0.0001.

our understanding of the molecular pathology of metabolic syndrome and hyperlipidemia-induced diastolic dysfunction and HFpEF.

## CONCLUSIONS

We present a novel murine model wherein diastolic dysfunction and classic symptoms of HFpEF are induced by pharmacological inhibition of combined with cardiac-specific overexpression of LDLR. The absence of obesity, hypertension, or diabetes suggests that lipotoxicity alone is sufficient to drive the phenotype, and this may represent a novel, more restricted HFpEF phenogroup related to but distinct from those of obesity with or without hypertension. The model may be applied to dissect pathways and mechanisms whereby lipotoxicity drives HFpEF and is especially relevant to high-incidence arrhythmia and sudden death.

## ARTICLE INFORMATION

Received June 20, 2022; accepted July 26, 2022.

### Affiliations

Department of Medicine, Division of Cardiology (M.W., J.M.C.C., C.I.I., G.L., J.J.G., L.A.S.); Interdisciplinary Stem Cell Institute (M.W., J.M.C.C., C.I.I., G.L., A.K., K.Y., R.K.-T., L.T., J.M.H., L.A.S.); Department of Medical Education (G.S.); Departments of Pathology and Pediatrics (A.G.S.), and Division of Endocrinology, Diabetes and Metabolism, Diabetes Research Institute (A.M.), University of Miami Leonard M. Miller School of Medicine, Miami, FL; Cullen Eye Institute (K.A.W.) and Integene International LLC, Houston, TX (K.A.W.).

### Acknowledgments

We thank the Analytical Imaging Core Facility at the University of Miami Miller School of Medicine for the VS120 Slide Scanner (grant 1S10OD023579-01 from the NIH), and the Penncore and NHLBI Gene Therapy Resource

Program (GTRP) for making the Adeno-associatedvirus9s used in this project.

### Sources of Funding

This research was funded by grants from the National Institute of Health (NIH) (1R01HL140468) and the Miami Heart Research Institute to LS. MW is recipient of NIH Diversity Supplement Award (R01HL140468-03S1). AM is funded by the Diabetes Research Institute Foundation. KW is funded by R24EY028764 and R43EY031238 from the NIH. JH is funded by 1R01 HL13735, 1R01 HL107110, 5UM1 HL113460, 1R01 HL134558, 5R01 CA136387 (from the NIH), W81XWH-19-PRMRP-CTA (from the Department of Defense), and the Starr, Lipson, and Soffer Family Foundations. JG is funded by 5R01HL155718-02 and 5R01HL145165-03 (from the NIH).

### Disclosures

JH is listed as a co-inventor on patents on GHRH analogs, which were assigned to the University of Miami and Veterans Affairs Department. JH previously owned equity in Biscayne Pharmaceuticals, licensee of intellectual property used in this study. Biscayne Pharmaceuticals did not provide funding for this study. JH reported having a patent for cardiac cell-based therapy. He holds equity in Vestion Inc. and maintains a professional relationship with Vestion Inc. as a consultant and member of the Board of Directors and Scientific Advisory Board. JH is the Chief Scientific Officer, a compensated consultant and advisory board member for Longeveron, and holds equity in Longeveron. JH is also the co-inventor of intellectual property licensed to Longeveron. Longeveron LLC and Vestion Inc. did not participate in funding this work. JH's relationships are disclosed to the University of Miami, and a management plan is in place.

## REFERENCES

- Mishra S, Kass DA. Cellular and molecular pathobiology of heart failure with preserved ejection fraction. *Nat Rev Cardiol*. 2021;18:400–423. doi: 10.1038/s41569-020-00480-6
- Powell-Wiley TM, Poirier P, Burke LE, Despres JP, Gordon-Larsen P, Lavie CJ, Lear SA, Ndumele CE, Neeland IJ, Sanders P, et al. Obesity and cardiovascular disease: a scientific statement from the American Heart Association. *Circulation*. 2021;143:e984–e1010. doi: 10.1161/CIR.0000000000000973
- Leggat J, Bidault G, Vidal-Puig A. Lipotoxicity: a driver of heart failure with preserved ejection fraction? *Clin Sci (Lond)*. 2021;135:2265–2283. doi: 10.1042/CS20210127

4. Hahn VS, Knutsdottir H, Luo X, Bedi K, Margulies KB, Haldar SM, Stolina M, Yin J, Khakoo AY, Vaishnav J, et al. Myocardial gene expression signatures in human heart failure with preserved ejection fraction. *Circulation*. 2021;143:120–134. doi: [10.1161/CIRCULATIONAHA.120.050498](https://doi.org/10.1161/CIRCULATIONAHA.120.050498)
5. Patel M, Rodriguez D, Yousefi K, John-Williams K, Mendez AJ, Goldberg RB, Lymperopoulos A, Tamariz LJ, Goldberger JJ, Myerburg RJ, et al. Osteopontin and LDLR are upregulated in hearts of sudden cardiac death victims with heart failure with preserved ejection fraction and diabetes mellitus. *Front Cardiovasc Med*. 2020;7:610282. doi: [10.3389/fcvm.2020.610282](https://doi.org/10.3389/fcvm.2020.610282)
6. Irion CI, Williams M, Capcha JC, Eisenberg T, Lambert G, Takeuchi LM, Seo G, Yousefi K, Kanashiro-Takeuchi R, Webster KA, et al. Col4a3(−/−) mice on Balb/C background have less severe cardiorespiratory phenotype and SGLT2 over-expression compared to 129x1/SvJ and C57Bl/6 backgrounds. *Int J Mol Sci*. 2022;23:6674. doi: [10.3390/ijms23126674](https://doi.org/10.3390/ijms23126674)
7. Dunkley JC, Irion CI, Yousefi K, Shehadeh SA, Lambert G, John-Williams K, Webster KA, Goldberger JJ, Shehadeh LA. Carvedilol and exercise combination therapy improves systolic but not diastolic function and reduces plasma osteopontin in Col4a3(−/−) Alport mice. *Am J Physiol Heart Circ Physiol*. 2021;320:H1862–H1872. doi: [10.1152/ajpheart.00535.2020](https://doi.org/10.1152/ajpheart.00535.2020)
8. Korolenko TA, Johnston TP, Tuzikov FV, Tuzikova NA, Pupyshv AB, Spiridonov VK, Goncharova NV, Maiborodin IV, Zhukova NA. Early-stage atherosclerosis in poloxamer 407-induced hyperlipidemic mice: pathological features and changes in the lipid composition of serum lipoprotein fractions and subfractions. *Lipids Health Dis*. 2016;15:16. doi: [10.1186/s12944-016-0186-7](https://doi.org/10.1186/s12944-016-0186-7)
9. van Veldhuisen DJ, van Woerden G, Gorter TM, van Empel VPM, Manintveld OC, Tieleman RG, Maass AH, Vernooy K, Westenbrink BD, van Gelder IC, et al. Ventricular tachyarrhythmia detection by implantable loop recording in patients with heart failure and preserved ejection fraction: the VIP-HF study. *Eur J Heart Fail*. 2020;22:1923–1929. doi: [10.1002/ehf.1970](https://doi.org/10.1002/ehf.1970)
10. Amin HZ, Amin LZ, Wijaya IP. Galectin-3: a novel biomarker for the prognosis of heart failure. *Clinul Med*. 2017;90:129–132. doi: [10.15386/cjmed-751](https://doi.org/10.15386/cjmed-751)
11. Rosenkranz S, Howard LS, Gombert-Maitland M, Hoepfer MM. Systemic consequences of pulmonary hypertension and right-sided heart failure. *Circulation*. 2020;141:678–693. doi: [10.1161/CIRCULATIONAHA.116.022362](https://doi.org/10.1161/CIRCULATIONAHA.116.022362)
12. Salloum G, Crawford JJ, Dryden S, Meador AG, Wesley RE, Klippenstein K. Lower eyelid ectropion secondary to over-the-counter treatment of xanthelasma. *Ophthalmic Plast Reconstr Surg*. 2022;38:e25–e28. doi: [10.1097/IOP.0000000000002070](https://doi.org/10.1097/IOP.0000000000002070)
13. Schiattarella GG, Altamirano F, Tong D, French KM, Villalobos E, Kim SY, Luo X, Jiang N, May HI, Wang ZV, et al. Nitrosative stress drives heart failure with preserved ejection fraction. *Nature*. 2019;568:351–356. doi: [10.1038/s41586-019-1100-z](https://doi.org/10.1038/s41586-019-1100-z)